Global Journal of Researches in Engineering
Electrical and Electronics Engineering
Volume 13 Issue 12 Version 1.0 Year 2013
Type: Double Blind Peer Reviewed International Research Journal
Publisher: Global Journals Inc. (USA)
Online ISSN: 2249-4596 & Print ISSN: 0975-5861

New Robust Energy Storage Devices for Deregulated AGC Problems

By J.Raja, C. Christober Aisr Rajan
National Power Training Insitute (CO), Ministry of Power, Govt. of india, India

Abstract - This paper presents a suitable mathematical model of Hydro-Thermal (H-T), Wind-Diesel (W-D) and Combined Cycle Gas Turbine (CCGT) system under deregulated environment. The variable power consumption as well as intermittent load variation may cause large fluctuations on system frequency. To reduce the system oscillations Superconducting Magnetic Energy Storage (SMES) and Capacitive Energy Storage (CES), which will supply and absorb active, reactive powers quickly, can be applied. In addition, variation of system parameters, load and unpredictable power demands cause various uncertainties in the system. Energy storage devices so far designed without considering such uncertainties may lose control effect. To enhance the robustness of storage devices, this paper focuses on a new SMES and CES robust frequency controllers are designed for three area power system. The coprime factorization method is used to represent the unstructured uncertainties in a system modeling. The structure of SMES and CES controller are the practical first order lead/lag compensator. To tune the controller parameters, the optimization problem is formulated based on loop shaping technique.

Keywords : capacitive energy storage, loop shaping control, particle swarm optimization, robust frequency controller, superconducting magnetic energy storage.

GJRE-F Classification : *FOR Code: 090607, 290903p*

New Robust Energy Storage Devices for Deregulated AGC Problems

J.Raja, C. Christober Aisr Rajan

Abstract - This paper presents a suitable mathematical model of Hydro-Thermal (H-T), Wind-Diesel (W-D) and Combined Cycle Gas Turbine (CCGT) system under deregulated environment. The variable power consumption as well as intermittent load variation may cause large fluctuations on system frequency. To reduce the system oscillations Superconducting Magnetic Energy Storage (SMES) and Capacitive Energy Storage (CES), which will supply and absorb active, reactive powers quickly, can be applied. In addition, variation of system parameters, load and unpredictable power demands cause various uncertainties in the system. Energy storage devices so far designed without considering such uncertainties may lose control effect. To enhance the robustness of storage devices, this paper focuses on a new SMES and CES robust frequency controllers are designed for three area power system. The coprime factorization method is used to represent the unstructured uncertainties in a system modeling. The structure of SMES and CES controller are the practical first order lead/lag compensator. To tune the controller parameters, the optimization problem is formulated based on loop shaping technique. The particle swarm optimization (PSO) is applied to solve the problem to achieve the controller parameters and also to optimize the Integral Controllers of three area power system in deregulated environment.

Keywords : capacitive energy storage, loop shaping control, particle swarm optimization, robust frequency controller, superconducting magnetic energy storage.

I. Introduction

Load Frequency Control (LFC) is a mechanism by which power generation and power demand are balanced. The frequency control is one of the most profitable ancillary services. This service is related to the short-term balance of energy and frequency of the power systems. The goal of LFC is to reestablish primary frequency regulation capacity, return the frequency to its nominal value and minimize unscheduled tie-line power flows between neighboring control areas. From the mechanisms used to manage the provision this service in ancillary markets, the bilateral contracts or competitive offers stand out [1]. In the past decade, the electrical industry has undergone deregulation and restructuring, when vertically integrated utilities were forced to split into separate independent Generation (GENCO), Transmission (TRANSCO) and distribution (DISCO) companies. There have been continuing efforts in design of LFC with better performance according to the change of environment in power system operation under deregulation using various optimal and robust control strategies during the recent years [2–4].

A simple, mathematical model of Heat recovery steam generator (HRSG), Steam turbine (ST), and pertinent controls are described and the model of a single-shaft CCPP is completed in [5]. Dynamics of combined cycle gas turbines to frequency deviations on an island electricity system is considered [6]. In [7] proposes the design and development of a new fuzzy GA predictive supervisory control strategy for gas turbines based on nonlinear predictions using the fuzzy model. Different gas turbine models are identified presented and discussed in [8]. The identified models are of different level of accuracy, suitable for different types of studies and have been utilized for different purposes in the past. However, these models are too complex and unsuitable for the use in large power system studies. In [7] has more detailed analysis of power system and governor behavior, especially for equipment specific studies and large frequency excursions, models.

In [9-10] compares various models and concluded that models have different level of accuracy. This study illustrates the usefulness and accuracy of frequency dependent model as well as the detailed model of gas turbines in CCPP, since these three models consider the IGV. One of the aim of this paper is to study the dynamic behavior of the CCGT in the presence of a frequency drop coordinated by energy storing devices like SMES/CES under deregulated environment. Detailed model which giving the available thermal power to the gas turbine and the steam turbine is modeled by algebraic equations. These equations are relating the adiabatic compression and expansion, as well as to the heat exchange in the recovery boiler [11-13] and it is presented in Appendix-3.

Wind power systems are considered economically for supply of electrical energy to remote and isolated areas where utility lines are uneconomical to install due to high costs, right of way difficulties or environmental impacts [14,15]. Since wind power sources are naturally fluctuating or intermittent, they are generally integrated with the diesel generation [16]. Different technologies such as flywheel [17], Battery Energy Storage (BES), Superconducting Magnetic Energy Storage (SMES), etc., can be adopted to

Author : E-mail : rajaj1980@rediff.com

alleviate system frequency fluctuation in isolated systems. Finally, robust controller of SMES for frequency control in the hybrid wind-diesel power system has been presented in [18].

In [19] the power systems with three areas are considered, the simulation is implemented by using MATLAB/Simulink Program and MATLAB Fuzzy Logic Toolbox (FLT), to damp out the oscillations, due to instantaneous load perturbations as fast as possible. In [20] has detailed model for the simulation of the SMES system and this model is intended to provide guidelines for a detailed SMES device simulation in the power system as well as to provide a basis for comparison of various simulation tools, control strategies, algorithms and realization approaches.

References [21-22] made comprehensive mathematical model for the AGC of a two area interconnected hydrothermal power system fitted with SMES unit in either thermal or hydro area with generator rate constraints has been presented. It has been shown that these oscillations can be effectively damped out with the use of a small capacity SMES unit in either of the areas following a step load disturbance.

Similarly like SMES, CES is one of the alternate energy storage for control the frequency oscillations in power system, [23] proposes new incorporation of ultra-capacitor banks in an interconnected power system for improved load frequency control. In ref. [24] analyses the usage of energy storage devices shows that super-capacitors are best suited for short-term low power (<100kW) applications.

This paper proposes a new robust frequency controller of SMES, CES in a three area deregulated system. To take system uncertainties mentioned above into account in the control design, the normalized coprime factorization [26, 27] is applied to represent all unstructured uncertainties in the system modeling. The configuration of the frequency controller of SMES/CES is the first-order lead/lag compensator. The performance and stability conditions in the H∞ loop shaping method [28] are applied to formulate the optimization problem. To achieve the controller parameters, the Particle Swarm Optimization (PSO) [29-30] is used to solve the objective function.

II. Problem Formulation

Since the system under consideration is exposed to a small change in load during its normal operation, a linearized model is sufficient for its dynamic representation. Fig. 1 shows the small perturbation transfer function block diagram model of H-T system. SMES and CES conventional energy storage and proposed frequency controllers devices are fitted to either area 1 or 2 to examine its effect on the power system performance.

Fig. 2 shows the basic configuration of the hybrid W-D system. In addition to the random wind energy supply, it is assumed that loads with sudden change have been placed in this deregulated system. Variation of wind power and load change results in a serious problem of large frequency fluctuation in the system. Such frequency fluctuation severely affects the system stability. Furthermore, the life time of machine apparatus on the load side is reduced.

Fig 3(a) shows the model of CCGT, it consists of the power generation units and the control branches. The thermodynamic part giving the available thermal power to the gas turbine and the steam turbine is modeled by Algebraic Equations are given in Appendix-3, corresponding to the adiabatic compression and expansion, as well as to the heat exchange in the recovery boiler. These equations correspond to the block 'Algebraic equations of energy transform are in subsystem in Fig 3(b). The nominal parameters of these three power system data's are given in the Appendix 1.

First these three dynamics models are considered separately to design SMES and CES frequency controllers. The co-prime factorization method is used to represent the unstructured uncertainties in a system modeling. After designing the energy storage controllers for all these systems, these systems are combined and the effects of bilateral contracts are taken in to account. In the considered power system, each area contains two GENCOs, the GENCOs at the first areas include H-T, Second and Third area includes W-D and CCGT generating units respectively. After deregulation, to describe bilateral contract for three-area AGC, DISCO participation matrix used. The performance of the system is studied for different operating cases, in terms of the conventional controller gains optimized by PSO. Finally, obtained results are compared with conventional energy storage devices.

Fig. 5 (a) and (b) shows, the block diagram of SMES/CES consists of two transfer functions connected in series in [31]-[32], i.e. energy storage model and frequency controller. Both models are first order transfer function with time constant of TSMES=0.06s, TCES=0.056s both frequency controllers are first order lead/lag compensator and with three control parameters. Change in frequency deviation is the input signal to the controllers.

III. Proposed Control Design

This paper proposes a robust control design of energy storage frequency controllers in H-T, W-D and CCGT systems. The configuration of SMES, CES frequency controller's are1st-order lead/lag compensator [26]-[27]. The normalized co prime factor is used to model system uncertainties. The H∞ loop shaping technique is applied to formulate the

Global Journal of Researches in Engineering (F) Volume XIII Issue XII Version I Year 2013

optimization problem of controller parameters. The PSO referred in [29]-[30] is employed to solve the problem.

Proposed algorithm is summarized as

i. Specify weighting function W_1 and W_2, shape the nominal plant Gs.
ii. Evaluate the γ_{min} using (3). If $\gamma_{min} \geq 4$, then go to step (i), adjust the weight function.
iii. Generate the objective for PSO.
iv. Initialize the PSO parameters.
v. Randomly generate the population and evaluate the objective function of each individual.
vi. Select the best individual in the current generation and update the velocity factor then go to step iv. Repeat the process until the last iterations reached.

H∞ Loop shaping is a feasible method for designing robust controller, however the controller design by this method is complicated and higer order. To overcome this problem this paper proposes an algorithm compared with PSO based fixed structure H∞ loop shaping control technique for designing controller, by this method a simple structured and robust controllers are achieved. The objective of the control design is to optimize three control parameters using PSO, so that the resulted controller is robust to system uncertainties. Based on the H∞ loop shaping control the optimization problem can be formulated subsequently the design procedure is divided in to (vi) steps as follows:

i. *Selection of the Weighing Functions*

H∞ Loop requires only a desired open loop shape in frequency domain. In this work pre compensator W_1 and Post compensator W_2 are used to shape the transfer function of the plant Gs in [18], [31] shown in figure 4, so that specification in frequency domain is achieved. The most crucial part of the design procedure is to find the appropriate weighing matrix. In this work W_1 and W_2 are designed by a systematic procedure by [26] and it has given excellent result. The shape of the weight is designed by the closed loop design specification. The faster settling time can be achieved with a high loop cross over frequency and a good ε.

$$W_1 = K_W \frac{S+a}{S+b}, \; W_2 = 1 \qquad (1)$$

Where Kw, a and b are positive values. Because, the frequency control problem is in a vicinity of low frequency (<1Hz), W_1 is set as a high pass filter (a<b). The W_2 is used to reject the high frequency noises and this is a common practice in real application and it can be chosen as unity matrix in [26]. Here the linearised H-T, W-D and CCGT models are used in this simulation. Now the shaped plant Gs is established by weighting functions W_1 and W_2 . The weighting functions are chosen as:

$$W_1 = 296\frac{(0.786S+7.0)}{(S+0.085)}, \; W_2 = 1 \text{ for H-T at this point } \gamma_{min} \text{ is } 1.8875$$

$$W_1 = 947\frac{(S+167)}{(S+544)}, \; W_2 = 1 \text{ for W-D at this point } \gamma_{min} \text{ is } 2.5496.$$

$$W_1 = \begin{bmatrix} 1277\dfrac{S+324}{S+329} & 0 \\ 0 & 1279\dfrac{S+335}{S+360} \end{bmatrix}, \; W_2 = 1 \text{ for CCGT at this point } \gamma_{min} \text{ is } 3.1256$$

$$\gamma_{min} \leq 4.0 \text{ for all the three systems.}$$

ii. *Formulate the Shaped Plant GS*

The figure 4 shows W_1 and W_2 that are employed to form the shaped plant G_s. $G_s = W_2 G W_1$, which is enclosed by the solid line. The proposed robust controller $K = W_1 K W_2$ is enclosed by the dotted line where K∞ is the H∞ controller.

iii. *Robust Stability margin of the system*

In this approach, the shaped plant is formulated as Normalized Co prime factorization method, which separates the plant Gs in to normalized nominator Ns and denominator Ms factors. The variation of system parameters, unpredictable load demand and fluctuation in real power are considered as uncertainties. These uncertainties cannot be clearly represented by mathematical equations. So co prime factorization methods is used to represent these uncertainties. If the shaped plant Gs is expressed in the form of:

$$G_s = W_2\, G\, W_1 = N_s M_s^{-1} \qquad (2)$$

Then perturbed plant Gs is defined as

$$G_\Delta = \{(M_S + \Delta M_S)^{-1}\,(N_S + \Delta N_S) : \|\, \Delta N_S\, \Delta M_S \,\| \leq 1/\gamma\} \qquad (3)$$

Where ΔM_s, and ΔN_s are stable unknown transfer functions which represent unstructured uncertainties in the nominal plant model G. Based on this definition, the robust control problem can be established by GΔ and K. The objective of robust control design is to stabilize not only the nominal plant G, but also the family of perturbed plant GΔ. In (3) 1/γ is defined as the robust stability margin ε. The ε can take the value between 0 and 1. ε is an indicator of success of the design procedure. If the value ε is small, it means that the desired loop shape and robust stability requirements cannot be achieved simultaneously. In this case designer should reshape the open loop scaled plant. The theoretical basis for H∞ loop shaping is that K does not modify the desired loop shape significantly at low and high frequencies, if the achieved ε is not too small, thus shaping of the open loop plant G corresponds to shaping the loop gain GK and KG. In contrast with the conventional loop shaping, the control engineer does not need to shape of the phase of G explicitly. It has been shown that a value of ε >0.25 to 0.3 is satisfactory for a SISO system in the same way gain margin is ± 6 dB, and phase margin of 45°.

The value of γmin can be easily calculated from

$$\gamma_{min} = (1 + \lambda_{max}(XZ))^{1/2} \quad (4)$$

Where λ_{max} (XZ) denotes the maximum Eigen value of XZ. For minimal state space realization (A, B, C, D) of Gs, the values of X and Z are unique positive solutions to the generalized control algebraic Riccati equation.

$$(A-BS^{-1}D^TC)^TX + X(A-BS^{-1}D^TC) - XBS^{-1}B^TX + C^TR^{-1}C = 0 \quad (5)$$

and the generalized filtering algebraic Riccati equation

$$(A-BS^{-1}D^TC)Z + Z(A-BS^{-1}D^TC)^T - ZC^TR^{-1}CZ + BS^{-1}B^T = 0 \quad (6)$$

Where $R=I+DD^T$ and $S=I+D^TD$. Note that no iteration on γ is needed to solve for γ_{min}. To ensure the robust stability of the nominal plant, the weighting function is selected so that $\gamma_{min} \leq 4.0$. if γ_{min} is not satisfied then go to step (i) and adjust the weighting functions. Thus the shaped plant is established at this point the values for H-T system the value of γ_{min} =3.1256, similarly W-D γ_{min} =2.5496, and CCGT γ_{min} = 1.8875.

iv. *Formulate the Objective Function for PSO Optimization function*

In this study, the performance and robust stability conditions in H∞ loop shaping design approach are adopted to design a robust frequency controller K. The frequency controller is represented by:

$$K = K_{SMES}\frac{(1+ST_{SMES1})}{(1+ST_{SMES2})} \quad (7)$$

$$K = K_{CES}\frac{(1+ST_{CES1})}{(1+ST_{CES2})} \quad (8)$$

The control Parameters for SMES, CES frequency controllers are KSMES, T_{SMES1}, T_{SMES2} and KCES, T_{CES1}, T_{CES2} are optimized by PSO. The objective function is derived based on the following concept. The designed controller K can be represented as

$$K = W_1 K_\infty W \quad (8)$$

or

$$K_\infty W_2 = W_1^{-1} \quad (9)$$

Selecting W_2=1 yields

$$K_\infty = W_1^{-1} K \quad (10)$$

Using MATLAB program Gs is formulated.

The necessary and sufficient condition of the designed robust controller K is

$$\left\| \begin{bmatrix} I \\ K_\infty \end{bmatrix} (I - G_s K_\infty)^{-1} [I \quad G_s] \right\|_\infty \leq \gamma \quad (11)$$

Substituting (10) into (11) yields

$$\left\| \begin{bmatrix} I \\ W_1^{-1}K \end{bmatrix} (I - G_s W_1^{-1} K_\infty)^{-1} [I \quad G_s] \right\|_\infty \leq \gamma \quad (12)$$

Equation (12) implies that if the ∞ -norm of transfer function matrix in the left side is lower than γ, the robust controller *K* can be obtained. As a result, the ∞ -norm of the left side term in (12) can be used to formulate the optimization problem as

$$\text{Minimize} \left\| \begin{bmatrix} I \\ W_1^{-1}K \end{bmatrix} (I - G_s W_1^{-1} K_\infty)^{-1} [I \quad G_s] \right\|_\infty \leq \gamma \quad (13)$$

Subject to

System	***SMES***	***CES***
H-T	$0 \leq K_{SMES} \leq 0.65$, $0.01 \leq T_{SMES1} \leq 1.0$ $0.01 \leq T_{SMES2} \leq 1.0$	$0 \leq K_{CES} \leq 0.95$, $0.001 \leq T_{CES1} \leq 1.0$ $0.001 \leq T_{CES2} \leq 1.0$

CCGT	$1.0 \le K_{sm} \le 125.0$, $0.04 \le T_{Sm1} \le 1.0$, $0.01 \le T_{Sm2} \le 1.0$	$1.0 \le K_{CES} \le 150.0$, $0.05 \le T_{CES1} \le 1.0$, $0.001 \le T_{CES2} \le 1.0$
W-D	$1.0 \le K_{SMES} \le 50.0$, $0.001 \le T_{SMES1} \le 1.0$, $0.001 \le T_{SMES2} \le 1.0$	$0 \le K_{CES} \le 35.0$, $3.0 \le T_{CES1} \le 1.0$, $0.001 \le T_{CES2} \le 1.0$

v. *PSO Algorithm*

a) Initialize a population of the particles with random position and velocities.

b) Evaluate the objective function in (13) for each particle.

c) Compare the fitness value of each particle with it's the best position for each particle (P_{best}). The best fitness value among all the P_{best} is the best position of all particles in the group (G_{best}).

d) Update the velocity V_i and position of particle x_i by

$$V_{i+1} = w\, v_i + c_1\, rand_1\, (pbest - x_i) + c_2\, rand_2\, (pbest - x_i) \quad (14)$$

$$X_{i+1} = x_i + v_{i+1}$$

$$w = w_{max} - \frac{w_{max} - w_{min}}{iter_{max}}\, iter$$

Where c_1, c_2 are the cognitive and social acceleration factors. $rand_1$, $rand_2$ are the random numbers of range 0 to 1. W is the inertia weight factor. W_{min}, W_{max} are the minimum and maximum of inertia weight factors. Iter and $Iter_{max}$ are the iteration count and maximum iterations.

e) The maximum number of iteration is arrived, stop the process. Otherwise go to process (b). The proposed controller achieves good robust performance by applying two specified weighting functions. Although design of a fixed-structure controller is difficult because of its inherently non-convex nonlinear problem, the PSO algorithm simplifies this by searching for optimal solutions. Based on the concept of convention $H\infty$ loop shaping, only a single index, stability margin, γ is applied to indicate performance of the designed controller. Optimal stability margin γopt is found to be 3.1256 for H-T system, 2.5496 for W-D system and 1.8775 for CCGT.

vi. After running PSO algorithms for 100 to 150 iterations for all the three systems and the obtained values listed are Table-1, in the frequency response of the complicated controller in the conventional design, the proposed approach significantly improves practical control by simplifying the controller structure and reducing the controller order while retaining robust performance. This makes the proposed controller more practical and attractive.

IV. Restructured System for AGC with Three Area

Power system contains three areas, each area includes two GENCOs and two DISCOs as shown in Fig.6. In the system, any GENCOs in any area may supply both DISCOs in its user pool and DISCOs in other areas through tie-lines allowing electric power to flow between areas. The transactions have to be implemented through an independent system operator (ISO). The impartial entity, ISO has to control many of ancillary services, one of which is AGC. In deregulated environment, any DISCOs has the liberty to buy power at competitive prices from different GENCOs, which may or may not have contract in the same area as the DISCOs. For practice, GENCOs–DISCOs contract is proposed in [33] with DISCO participation matrix (DPM). Essentially, DPM gives the participation of a DISCO in contract with a GENCO, total of entries of column belong to DISCO1 of DPM is $\sum C_{Pij}=1$.

$$DPM = \begin{bmatrix} Cp_{11} & Cp_{12} & Cp_{13} & Cp_{14} & Cp_{15} & Cp_{16} \\ Cp_{21} & Cp_{22} & Cp_{23} & Cp_{24} & Cp_{25} & Cp_{26} \\ Cp_{31} & Cp_{32} & Cp_{33} & Cp_{34} & Cp_{35} & Cp_{36} \\ Cp_{41} & Cp_{42} & Cp_{43} & Cp_{44} & Cp_{45} & Cp_{46} \\ Cp_{51} & Cp_{52} & Cp_{53} & Cp_{54} & Cp_{55} & Cp_{56} \\ Cp_{61} & Cp_{62} & Cp_{63} & Cp_{64} & Cp_{65} & Cp_{66} \end{bmatrix}$$

Where Cp represents "contract participation factor". In the case of three-area power system, scheduled steady state power flow on any tie-line is given as follows:

$$\Delta P_{i\text{-}j\ scheduled} = [\text{Demands of DISCOs in area } j \text{ from GENCOs in area } i]-[\text{Demand of DISCOs in area } i \text{ from GENCOs in area } j] \quad (15)$$

and

$$\Delta P_{1scheduled}(k)=\Delta P_{1\text{-}2scheduled}(k)+a_{31}\Delta P_{3\text{-}1scheduled}(k) \quad (16)$$

$$\Delta P_{2scheduled}(k)=\Delta P_{2\text{-}3scheduled}(k)+a_{12}\Delta P_{1\text{-}2scheduled}(k) \quad (17)$$

$$\Delta P_{3scheduled}(k)=\Delta P_{3\text{-}1scheduled}(k)+a_{23}\Delta P_{2\text{-}3\ scheduled}(k) \quad (18)$$

Where $a_{12} \neq a_{23} \neq a_{31}$ are different and not equal to -1, because in this study it is taken as $P_{r1} \neq P_{r2} \neq P_{r3}$ such that P_{r1}, P_{r2} and P_{r3} are rated power of areas and k is sampling index. The error for the power defined in (16)-(18) is given as follows:

$$\Delta P_{i\ error}=\Delta P_{i\ actual}-\Delta P_{i\ scheduled} \quad (19)$$

The error signal is used to generate its ACE signals in the steady state as follows:

$$ACE_i = B_i \Delta f_{ierror} + \Delta P_{ischeduled}\,; where\ i=1,2,3 \quad (20)$$

Equation of the considered power system including two areas is given in steady state form as follows:

$$\dot{X}(t) = AX(t) + BU(t) \quad (21)$$

Where X is sate vector, U is the demands of DSICOs.

V. PSO Application for Parameter Optimization

Fig 1 to 3, represents the detailed transfer function block of an area with diverse source of electric power generation namely thermal, hydro, gas and Wind-Diesel. The uncontrolled three area power system is shown in fig 6. The Thermal, Hydro, Gas and Wind-Diesel based units are presented by respective single plant dynamics under normal operating conditions, there is no mismatch between generation and load. The total generation in units 1,2 and 3 are given by:

$$PG = PG_{1(HT)} + PG_{2(CCGT)} + PG_{3(W-D)} \quad (22)$$

$$\left.\begin{aligned} PG_1 &= PG_{(H1)} + PG_{(T2)} \\ PG_2 &= PG_{(CCGT1)} + PG_{(CCGT2)} \\ PG_3 &= PG_{(W-D1)} + PG_{(W-D2)} \end{aligned}\right\} \quad (23)$$

The speed changer signal is given by

$$\left.\begin{aligned} \Delta P_{C(T)} &= K_{P(T)} ACE + K_{I(T)} \int (ACE_i)dt \\ \Delta P_{C(H)} &= K_{P(H)} ACE + K_{I(H)} \int (ACE_i)dt \\ \Delta P_{C(T)} &= K_{P(CCGT)} ACE + K_{I(CCGT)} \int (ACE_i)dt \\ \Delta P_{C(T)} &= K_{P(W-D)} ACE + K_{I(W-D)} \int (ACE_i)dt \end{aligned}\right\} \quad (24)$$

$$ACE_i = B\Delta f_i + \Delta P_{tie} \quad (25)$$

From (14), PSO algorithm updates the velocity for each particle then adds that velocity to the particle position or values. Velocity updates are influenced by both the best global solution associated with the lowest cost ever found by a particle and the best local solution associated with the lowest cost in the present population. If the best local solution has a cost less than the cost of the current global solution, then the best local solution replaces the best global solution. The particle velocity is reminiscent of local minimization that uses derivative information, because velocity is the derivative of position. The advantages of PSO are that it is easy to implement and there are few parameters to adjust. The PSO is able to tackle tough cost function with many local minima. In this problem PSO is used to optimize the gains of conventional PI controller with (ISE+ITAE) performance index as fitness function. The performance index is given by:

$$ISE = \Delta f_1^2 + \Delta f_2^2 + \Delta f_3^2 + \Delta P_{tie12} + \Delta P_{tie23} + \Delta P_{tie31} \quad (26)$$

$$ITAE = t(|\Delta P_{tie12}| + |\Delta P_{tie23}| + |\Delta P_{tie31}| + |\Delta f_1^2| + |\Delta f_2^2| + |\Delta f_3^2|) \quad (27)$$

$$\eta_{ISE+ITAE} = \int (ISE + ITAE)dt \quad (28)$$

VI. Result Discussions

Typical examples of three area power systems are considered for the simulation. The initial values of the performance indices were obtained by carrying out simulation of the system over a period of 150s with AGC gain parameters obtained from randomly selected initial population. The values were used to produce next generation of individuals and procedure is repeated until the population has converged to some minimum value of the performance index. The parameters for PSO process are given in Appendix-2. The three area system with diverse sources of power system under deregulated environment is simulated for different cases with 1% step load perturbation in either of the area.

Case 1

During the study, error signals Δf_1, Δf_2, Δf_3 and ΔP_{tie} (i.e 1-2,2-3,3-1) are required for the controller is transferred to PSO algorithm. All positions of particles on each dimension area clamped in limits which are specified by the user, and the velocities are clamped to the range [V_{min},V_{max}] given in [30] and a step increase in demand of 0.01p.u kW is applied to area1,2 and 3. The frequency deviation and tie line power signals are shown in fig.7. The PI value which was obtained by the PSO algorithm is compared with that of the one derived from Zeigler-Nichols method in various perspectives, namely robustness and stability, performance and the optimum values are tabulated in 2.

Fig 7 reveals that there is a substantial improvement in the time domain specification. The proposed PSO controller is proved better than conventional controller tuned by Ziegler method. In addition, the proposed controller is very simple and easy to implement since it does not requires many information about system parameters. The typical three area has been simulated for different scheduled generations under different load conditions with the variation of 25% from the nominal value in either area and the scheduled power generation from H-T, W-D and CCGT are adjusted to match the system normal operating load. But when the variation of system parameters, unpredictable power demands and fluctuation under these case, CCGT the acceptable speed variation is about 96% to 104% from their nominal values are greatly affects the system stability and system temperature increases which reduces the life of the CCGT equipment. For the case of W-D, wind is factor it will not always constant particularly, when the W-D connected the deregulated environment, the diesel system improves the stability only some acceptable range and diesel time constant is somehow high so again there is a problem of stability issues coming in to the picture.

First, a 0.01 pukW step increase in any one of the area in deregulated system at t = 0.0 s. Fig.8 (a),(b) and (c) shows the bar chart comparative analysis between % load variations with respect to Ts, Mp. Without SMES & CES, the system frequency highly oscillates, the deregulated three areas has very high Ts, Mp and high frequency oscillations and these oscillations about 140 sec in H-T, 100 sec in CCGT and 80 sec in W-D systems to reach zero. This indicates that the PSO controllers are not able to work well. On the other hand, the peak frequency deviation is reduced significantly and returns to zero within shorter period in case without or with the presence of energy storage devices.

Case 2

The optimisation algorithms used to reduces the damping of oscillations but has been proved that the AGC alone may not be sufficient to suppress these oscillations. With recent advances in high temperature superconductor materials, and power electronics and control techniques, the SMES/CES system, which combines the superconducting conductors and the power electronics converters, has become an important issue in electrical engineering. The installed SMES/CES system successfully damped the emerging 0.35Hz low frequency oscillation that had ever occurred on this transmission line and improved the stability of the transmission line.

Case 3

The validity of SMES, cES for power system dynamics performance improvement has been widely reported in [10]-[18]. Their applications in real power system have invited problems from the view point of operation, maintenance and cost involvement but capacitive energy storage (CES) is a better choice to damp out power system oscillations, following any perturbation in power system. Thus a corrective measure against power system perturbation, CES plays an important role to damp out local modes of oscillations.

Case 4

Comparative analysis: From the fig.9 shows bar chart shows the settling time, peakover shoot performance of proposed SMES and CES are close to each other in the context of transient analysis particularly under deregulated environment. But CES is practically maintenance free, it does not impose any environmental problem, and it is quite simple and less expensive. CES damping effects are slightly better than SMES when variation in load.

Case 5

The system parameter variations can be defined in uncertainties. To compare the performance of proposed SMES and CES under variations of system parameters in the presence of random load variations. The values of settling time for all the by changing H-T, CCGT and W-D parameters are presented in table II and it shows that three area parameters are varied 25% from their normal values. The Ts values for three areas with conventional SMES/CES largely increase/decreases the above mentioned parameter variations. In contrast, the Ts values of three areas with proposed SMES/CES are lower and slightly changed. The values in case of conventional SME/CES highly increase when all the system parameter decreases. This implies that conventional SMES/CES is very sensitive to the variation of system parameters. The proposed SMES/CES is very robust to the variations of system parameters under this random load changes.

VII. Conclusion

i. Modified AGC after deregulation, is an important issue in power system. AGC of a three area power system having power generation from Hydro Thermal sources in area-1, two Wind-Diesel turbines in area-2 and two combined cycle gas turbines in area-3 has been studied and ACE parameters are optimized for an appropriate performance index by using PSO.

ii. Further to improve the system performance, particularly with the presence of uncertainties. In this paper new SMES and CES robust frequency controllers are successfully implemented in three area power system. Finally comparative studies have been made between two energy storage frequency controllers and compared with the work published in ref [18] and [33].

iii. H∞ loop shaping is a feasible method for designing robust controllers, however the controller design by this method is complicated and higher order. To overcome this problem, we propose an algorithm called PSO based fixed structure H∞ loop shaping control to design a robust controller.

iv. By this method a simple structured robust controllers are designed, from this study it is found that this work may seems to be quite simple and easy to analyze in real power system. It has given very good results in terms of performance and stability.

v. The Simulation result clearly shows that proposed method is robust to change in system parameters and it has given better performance than conventional PI, SMES and conventional CES at all the Operating conditions. Performance of proposed robust frequency controllers, SMES and CES are close to each other in the context of transient analysis. But CES is practically maintenance free, it does not impose any environmental problem, and it is quite simple and less expensive. CES damping effects slightly better than SMES when variation in load for LFC problem in deregulated environment.

Appendix 1

Wind Diesel System:

$\mathbf{P_R}$ = 350 kW, $\mathbf{H_W}$ = 3.5 s, $\mathbf{H_D}$ = 8.5 s, $\mathbf{K_{fc}}$ = 16.2 Hz/pu kW, $\mathbf{K_D}$ = 16.5 Hz/pu Kw, $\mathbf{K_{P2}}$ = 1.25, $\mathbf{K_{P3}}$ = 1.4, $\mathbf{T_{P1}}$ = 0.6 s, TP2 = 0.041 s, $\mathbf{K_{PC}}$ = 0.08, $\mathbf{K_{PI}}$ = 4.0, $\mathbf{K_{PP}}$ = 1.5.

CCGT Data:

$\mathbf{T_{io}}$ =303 K, $\mathbf{T_{do}}$=390 C, $\mathbf{T_{fo}}$=1085 C, $\mathbf{T_{eo}}$=532 C, $\mathbf{P_{ro}}$=11.5, $\mathbf{\Gamma}$=1.4, $\mathbf{\eta_c}$=0.85, $\mathbf{\eta_t}$=0.85, $\mathbf{K_0}$=0.00303 (1/K), $\mathbf{K_1}$=0.000428 (1/K), **R**=0.04, $\mathbf{T_g}$=0.05 s, $\mathbf{K_4}$=0.8, $\mathbf{K_5}$=0.2, $\mathbf{T_3}$=15 s, $\mathbf{T_4}$ =2.5 s, $\mathbf{T_5}$=3.3 s, $\mathbf{T_t}$=0.4699 s, $\mathbf{T_{c\ max}}$=1.1 s, $\mathbf{T_{c\ min}}$=0 s, $\mathbf{F_{d\ max}}$=1.5, $\mathbf{F_{d\ min}}$=0, $\mathbf{K_3}$=0.77, $\mathbf{K_6}$=0.23, $\mathbf{T_v}$=0.05 s, $\mathbf{T_f}$=0.4 s, $\mathbf{T_6}$=60 s, $\mathbf{g_{max}}$=1.001, $\mathbf{g_{min}}$=0.73, $\mathbf{T_w}$=0.4699 s, $\mathbf{T_b}$=20 s, $\mathbf{T_{cd}}$=0.2 s, $\mathbf{T_m}$=5 s, $\mathbf{T_i}$=18.5 s, $\mathbf{T_{off}}$=0.01 s.

H-T Data:

$\mathbf{P_{r1}}$=$\mathbf{P_{r2}}$= 2000 MW, $\mathbf{H_1}$= $\mathbf{H_2}$= 5 s, **D**=8.33X10^{-3}pu.MW/Hz, $\mathbf{K_r}$=0.5, $\mathbf{R_1}$= $\mathbf{R_2}$=2.4 Hz/pu.MW, $\mathbf{T_r}$=10 s, $\mathbf{K_{p1}}$ =$\mathbf{K_{p2}}$=120 Hz/pu.MW, $\mathbf{T_{p1}}$=20 s, $\mathbf{T_{12}}$=0.86pu.MW/Radian, **f** = 60 Hz, $\mathbf{T_w}$=1.0 s, $\mathbf{a_{12}}$ = -1, $\mathbf{T_g}$=0.08 s, $\mathbf{T_t}$=0.3 s.

Global Journal of Researches in Engineering (F) Volume XIII Issue XII Version I Year 2013

Appendix-2

List of PSO parameters;

Number of particle – 20

Fitness function: $1/(1+(ISE+ITAE))$

Particle size: 14

Number of iteration: 100

C_1: 02

C_1: 02

Inertia Weight (w): decreasing from 0.9 to 0.2.

Appendix-3

$$X=\left(P_r\right)^{\frac{\gamma-1}{\gamma}} \quad .....(A.1)$$

$$P_r=P_{ro}*W \quad ....(A.2)$$

$$X=\left(P_{ro}*W\right)^{\frac{\gamma-1}{\gamma}} \quad ....(A.3)$$

$$\eta_c=\frac{t_{d,is}-t}{t_d-t} \quad ....(A.4)$$

$$t_d=\frac{t_1(1+X-1)}{\eta_c} \quad ....(A.5)$$

$$W_f=\frac{W(t_f-t_d)}{(t_{fo}-t_{do})} \quad ....(A.6)$$

$$t_f=t_d+(t_{fo}-t_{do})\frac{W_f}{W} \quad ....(A.7)$$

$$\eta_t=\frac{t_{t,is}-t}{t_t-t} \quad ....(A.8)$$

$$t_e=\frac{t_f[l-(l-1)\eta_t]}{X} \quad ....(A.9)$$

$$E_g=K_o[(t_f-t_e)-(t_d-t_i)]W \quad ....(A.10)$$

$$E_S=K_1*t_e*W \quad ....(A.11)$$

$$T_f=\frac{t_f-273}{t_{fo}} \quad ....(A.12)$$

$$T_e=\frac{t_e-273}{t_{eo}} \quad ....(A.13)$$

$$P=E_g+E_S \quad ....(A.14)$$

References Références Referencias

1. Raineri R, Rios S, Schiele D. Technical and economic aspects of ancillary services markets in the electric power industry: an international comparison. *Energy Policy 2006*; 34(13):1540–55.
2. Bevrani H, Mitani Y, Tsuji K. Robust decentralized AGC in a restructured power system. *Energy Conversion Management 2004*; 45:2297–312.
3. Donde V, Pai A, Hiskens I A. Simulation and optimization in a LFC system after deregulation. *IEEE Trans Power System* 2001; 16(3); 481–489.
4. Elgerd O I. Electric energy system theory: an introduction. *New York: McGraw Hill*; 1971.
5. Kazuyoshi Kunitomi., Atsushi Kurita., Yasuyuki Tada., Satoru Ihara, William W. Price., Leon M. Richardson., and Gordon Smith. Modeling Combined-Cycle Power Plant for Simulation of Frequency Excursions. *IEEE trans on Power Systems;* Vol. 18, no. 2, May 2003; pp 724-729.

6. Gillian Lalor., Julia Ritchie., Damian Flynn., and Mark J. O'Malley. The Impact of Combined-Cycle Gas Turbine Short-Term Dynamics on Frequency Control. *IEEE Transactions on Power Systems;* vol. 20, no. 3, Aug 2005, pp 1456-1464.
7. Doris S´aez., Freddy Milla., and Luis S. Vargas. Fuzzy Predictive Supervisory Control Based on Genetic Algorithms for Gas Turbines of Combined Cycle Power Plants. *IEEE Transactions On Energy Conversion*; vol. 22, No. 3, September 2007; pp 689-696.
8. Soon Kiat Yee., Jovica V. Milanovic., and F. Michael Hughes. Overview and Comparative Analysis of Gas Turbine Models for System Stability Studies. *IEEE trans on Power Systems*, vol. 23; no. 1, Feb 2008; pp 108-118.
9. Masayuki Watanabe., Yuuya Ueno., Yasunori Mitani., Hiroyuki Iki., Yoshihisa Uriu., and Yasuhiro Urano. Development of a Dynamical Model for Customer's Gas Turbine Generator in Industrial Power Systems. *2nd IEEE Int. Con.on Power and Energy (PECon 08);* Dec1-3, 2008, Johor Baharu, Malaysia; pp 514-519.
10. H. E. M. A. Shalan., M. A. Moustafa Hassan., and A. B. G. Bahgat. Comparative Study On Modeling Of Gas Turbines In Combined Cycle Power Plants. *Proc. Int. Middle East Power Systems Conference (MEPCON'10), Cairo University, Egypt*, December 19-21, 2010; Paper ID 317; pp 970-976.
11. Gillian Lalor, Julia Ritchie, Damian Flynn, and Mark J. O'Malley. The Impact of Combined Cycle Gas Turbine Short-Term Dynamics on Frequency Control. *IEEE Trans. on Power Syst.,* Vol. 20, No. 3, August 2005: pp 1456-1464.
12. John Mantzaris, and Costas Vournas. Modeling and Stability of a Single-Shaft Combined Cycle Power Plant. *Int. J. of Thermodynamics*; Vol. 10 (No. 2) June 2007; pp 71-78.
13. G. Lalor and M. O'Malley. Frequency Control on an Island Power System with Increasing Proportions of Combined Cycle Gas Turbines. *Proc. IEEE Power tech Conf., Bologna, Italy*, Jun. 2003; pp 187-193.
14. Ackermann, T. Wind power in power systems. *John Wiley & Sons Ltd*; 2005.
15. Patel, M.R. Wind and solar power systems, design, analysis and operation. *2nd Edition, CRC Press*; 2006.
16. Lipman, N.H. Wind-diesel and autonomous energy systems. *Elsevier Science Publishers Ltd;* 1989.
17. Takahashi, R, and Tamura, J. Frequency stabilization of small power system with wind farm by using flywheel energy storage system. *Proc. of IEEE Int symp of Diagnostics for Electric Machines, Power electronics and Drives* 2007; pp.393-398.
18. Issarachai Ngamroo. Robust Frequency Control of Wind-Diesel Hybrid Power System Using Superconducting Magnetic Energy Storage. *Int Journal of Emerging Electric Power Systems*, Vol.10, Issue2, 2009 Article 3; pp 1-26.
19. Demiroren, E. Yesil. Automatic generation control with fuzzy logic controllers in the power system including SMES units. *Electrical Power and Energy Systems* 26 (2004); pp. 291–305.
20. IEEE Task Force on Benchmark Models for Digital Simulation of FACTS and Custom-Power Controllers, T&D Committee. Detailed Modeling of Superconducting Magnetic Energy Storage (SMES) System. *IEEE Transactions On Power Delivery*, Vol. 21, no.2, April 2006: pp 699-710.
21. Rajesh Joseph Abraham, D. Das, Amit Patra. Automatic generation control of an interconnected hydrothermal power system considering superconducting magnetic energy storage. *Electrical Power and Energy Systems* 29 (2007); pp. 571–579.
22. Akira Taguchi, Tadakazu Imayoshi, Takashi Nagafuchi, Takahiro Akine, Nobuhiro Yamada,and Hidemi Hayashi. A Study of SMES Control Logic for Power System Stabilization. *IEEE Transactions On Applied Superconductivity*, Vol.17, no.2, June 2007, pp 2343-2346.
23. Mairaj ud din Mufti, Shameem Ahmad Lone, Shiekh Javed Iqbal, Muzzafar Ahmad, Mudasir Ismail. Super-capacitor based energy storage system for improved load frequency control. *Electric Power Systems Research* 79, 2009; pp 226–233.
24. S. Kim, S. Sul. Control of rubber typed gantry crane with energy storage based on super capacitor bank. *IEEE Trans. Energy Conv. 21 (6)*, 2006; pp 1420–1427.
25. T. Kinjo, T. Senjyu, K. Uezato, H. Fujita, Output leveling of renewable energy by power electric double-layer capacitor applied for energy storage system, IEEE Trans. Energy Conv. 21 (1), 2006; 221–227.
26. Macfarlane, D.C., and Glover, K. Robust controller design using normalized coprime factor plant descriptions. *Lecture notes in control and information sciences Springer*,1990;vol. 138.
27. Muhammad Ejaz, M. Naeem Arbab and S. Waqar Shah. Weight Selection in H∞ Loop Shaping Using Lead/Lag Compensators. *2nd international conference on Emerging Technologies, Peshawar, Pakistan*; 13-14 November 2006; pp 319-324.
28. Skogestad, S, and Postlethwaite. Multivariable feedback control: analysis and design. *2nd edition, John Wiely*, 2005.
29. Russell Eberhart. A New Optimizer Using Particle Swarm Theory. *Prude school of Enginering and Technology, Indianapolis;* IN 46202-5160 (eberhart@engr.iupui.edu) and James Kennedy Bureau of Labor Statistics, Washington, DC 20212 (kennedyj @pol.ocsp.bls.gov).

30. Shigenori Naka, Takamu Genji, Toshiki Yura and Yoshikazu Fukuyama. A Hybrid Particle Swarm Optimization for distributing state estimation. *IEEE Transaction on Power system*, vol 18th; Feb 2003.
31. Boom, R.W., and Perterson, H. A superconducting energy storage for power systems. *IEEE Transactions on Magnetic*; vol.8, 1972; pp. 701-703.
32. Ngamroo, I., Cuk Supriyadi, A. N., Dechanupaprittha, S., and Mitani, Y. Power oscillation suppression by robust SMES in power system with large wind power penetration. *Physica C: Superconductivity and Its Applications*, vol. 469, no. 1, 2009, pp. 44-51.

Table 1 : PSO algorithms for 100 to 150 iterations for all the three systems and the obtained values listed below

System	SMES Frequency controller value			CES Frequency controller value		
	K_{SMES}	T_{sm1}	T_{sm2}	K_{CES}	T_{CES1}	T_{CES2}
CCGT	112	0.5875	0.6547	146.7	0.79250	0.8813
H-T	0.56	0.2782	0.3652	0.865	0.3659	0.5651
W-D	48.9	0.9547	0.5682	29.8	0.7657	0.4864

Table 2 : Different System Controller Values obtained from PSO Algorithm

System	SMES Frequency controller value			CES Frequency controller value		
	K_{SMES}	T_{sm1}	T_{sm2}	K_{CES}	T_{CES1}	T_{CES2}
CCGT	112	0.5875	0.6547	146.7	0.79250	0.8813
H-T	0.56	0.2782	0.3652	0.865	0.3659	0.5651
W-D	48.9	0.9547	0.5682	29.8	0.7657	0.4864

Table 3 : Various Gain Values Obtained from Conventional and PSO Controller for Three Different Areas

		AREA 1		AREA 2		AREA 3	
		Hydro	**Thermal**	**CCGT**	**CCGT**	**W-D**	**W-D**
Conventional Controller	K_P	3.7640	3.6514	0.0121	0.021	3.500	3.500
	K_I	0.6561	0.5583	0.6631	0.6631	0.785	0.785
PSO controller	K_P	3.3260	3.5439	0.0562	0.0671	3.6762	3.6732
	K_I	0.6879	0.5983	0.8454	6.8456	0.8364	0.8366

Table 4 : ±25% changing parameter from their typical values the system uncertainties are obtained

System Parameter variation from the nominal value		Three Area T_s Value with Proposed SMES			Three Area T_s Value with Proposed CES		
		Δf_1	Δf_2	Δf_3	Δf_1	Δf_2	Δf_3
1.CCGT Power System							
R (Nominal Value 0.04)		59	45	45	50	40	43
±25%	0.05/0.03	65	54	56	52	43	44
±15%	0.046/0.034	60	50	44	51	43	43
T_g (Nominal Value 0.05)		59	45	45	50	40	43
±25%	0.0625/0.0375	65	49	56	60	49	50
±15%	0.0575/0.0425	62	47	49	56	42	47
T_i (Nominal Value 18.5)		59	45	45	50	40	43
±25%	23.13/13.88	70	65	65	55	48	50
±15%	21.3/15.72	65	55	57	54	45	47
T_{cd} (Nominal Value 0.2)		59	45	45	50	40	43
±25%	0.25/0.15	59	45	45	50	40	43
±15%	0.23/0.17	59	45	45	50	40	43

T_m(Nominal Value 5)		59	45	45	50	40	43
±25%	6.25/3.75	66	60	60	51	42	44
±15%	5.75/4.25	65	59	58	49	40	42
2.W-D Power System							
H_w (Nominal Value 3.5)		59	45	45	50	40	43
±25%	4.375/2.626	66	60	60	51	42	44
±15%	4.025/2.975	65	59	58	49	40	42
H_D (Nominal Value 8.5)		59	45	45	50	40	43
±25%	10.625/7.225	70	55	56	52	43	45
±15%	9.775/7.225	65	50	56	51	42	45
K_{PI} (Nominal Value 4.0)		59	45	45	50	40	43
±25%	5.0/3.0	59	45	45	50	40	43
±15%	4.6/3.4	59	45	45	50	40	43
3. H-T Power System							
T_g (Nominal Value 0.08)		59	45	45	50	40	43
±25%	0.1/0.06	59	45	45	50	40	43
±15%	0.0925/0.0675	59	45	45	50	40	43
T_t (Nominal Value 0.3)		59	45	45	50	40	43
±25%	0.375/0.225	59	45	45	50	40	43
±15%	0.345/0.255	59	45	45	50	40	43
T_w (Nominal Value 1.0)		59	45	45	50	40	43
±25%	1.25/0.75	66	60	60	51	42	44
±15%	1.15/0.85	65	59	58	49	40	42
H (Nominal Value 5)		59	45	45	50	40	43
±25%	6.25/3.75	75	65	72	55	48	43
±15%	5.75/4.25	70	55	65	50	45	43

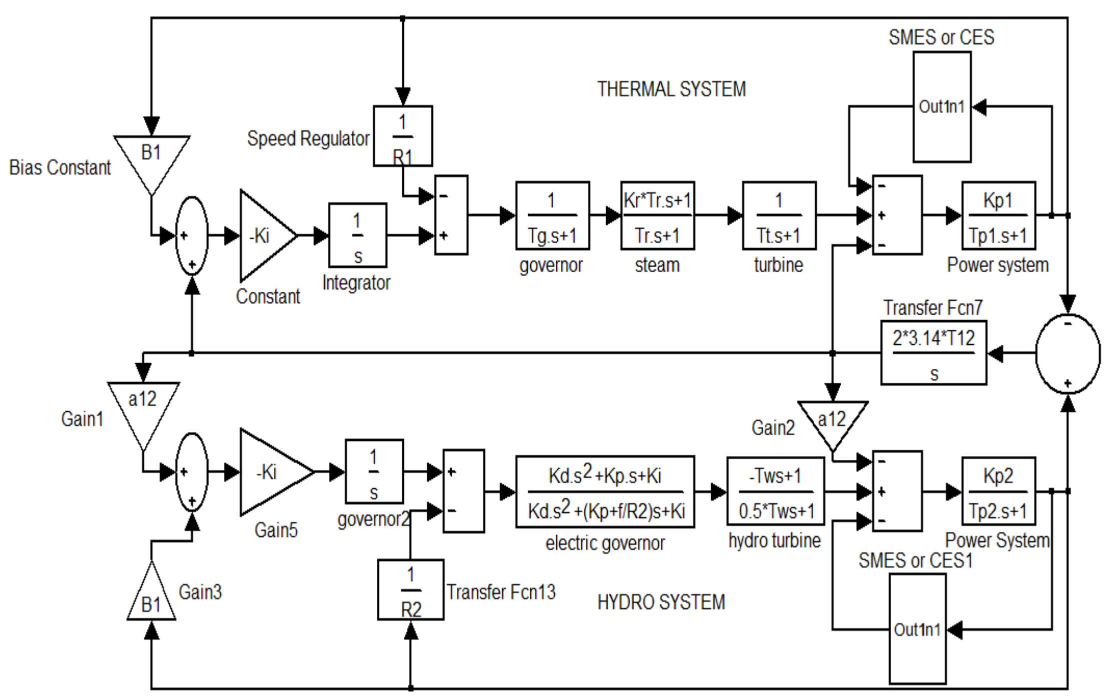

Fig. 1 : Transfer function model of H-T system co-ordinated with SMES or CES

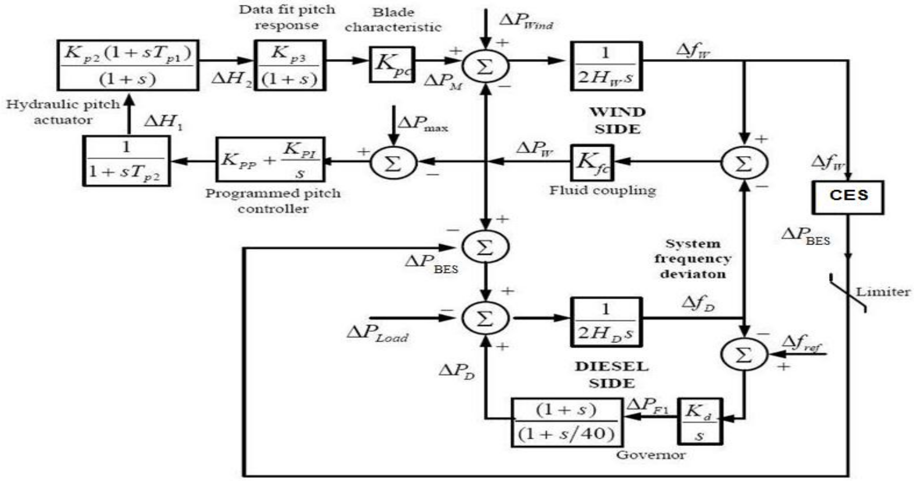

Fig. 2 : Transfer function model of W-D system co-ordinated with SMES or CES

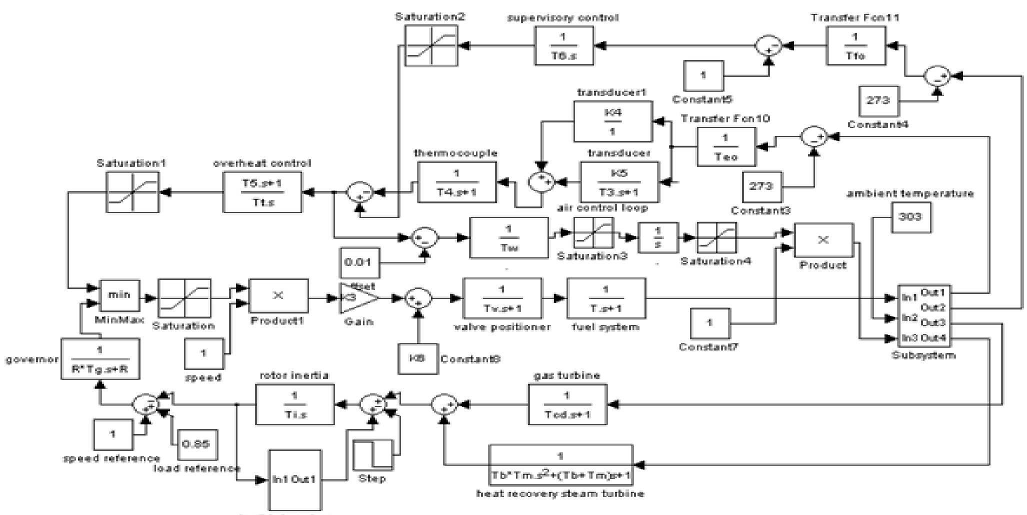

Fig. 3(a) : Transfer function model of CCGT system co-ordinated with SMES or CES

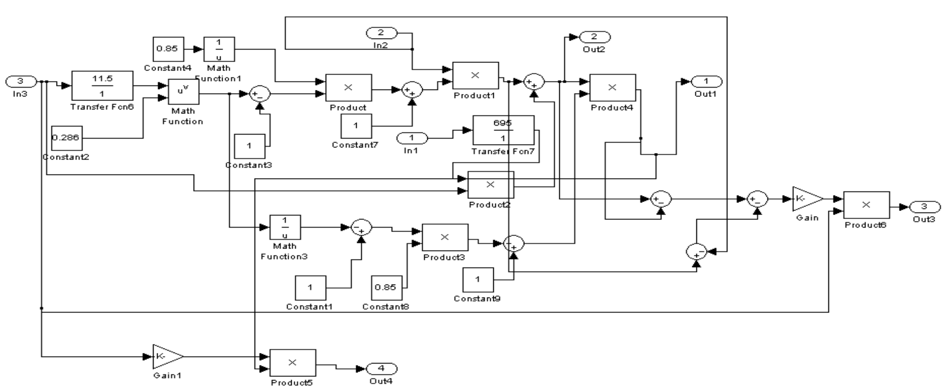

Fig. 3(b) : Sub System for adiabatic compression and expansion

Global Journal of Researches in Engineering (F) Volume XIII Issue XII Version I Year 2013

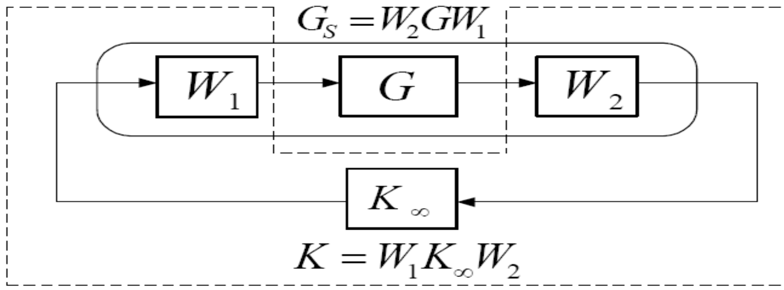

Fig.4 : Shaped Plant Gs and Robust Controller K

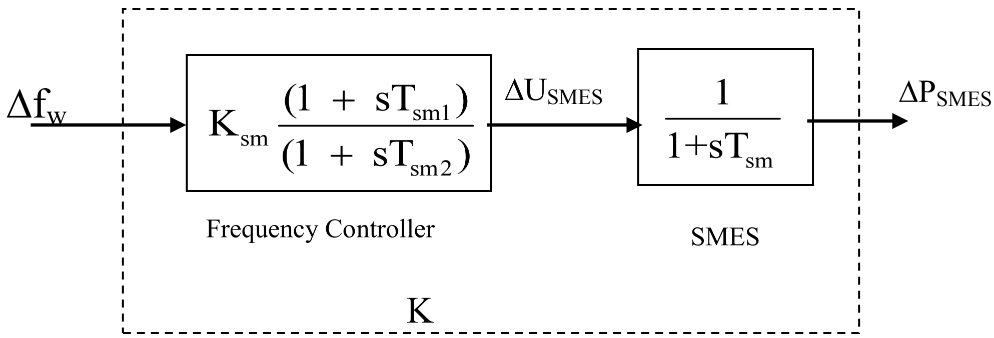

Fig. 5(a) : Block diagram of SMES with Frequency Controller

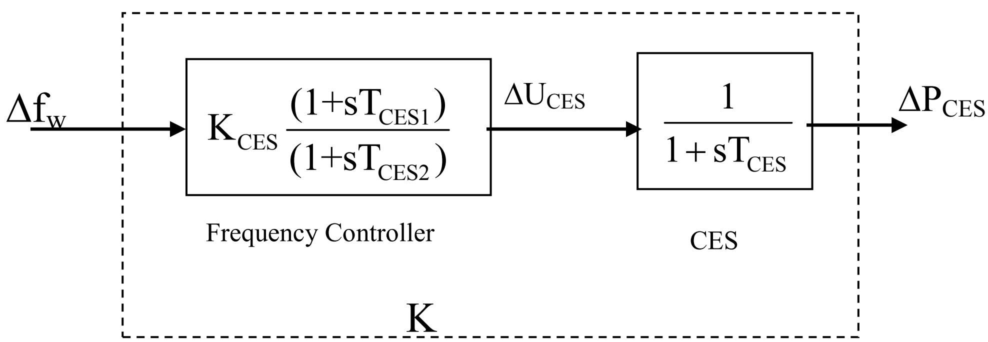

Fig. 5(b) : Block diagram of CES with Frequency Controller

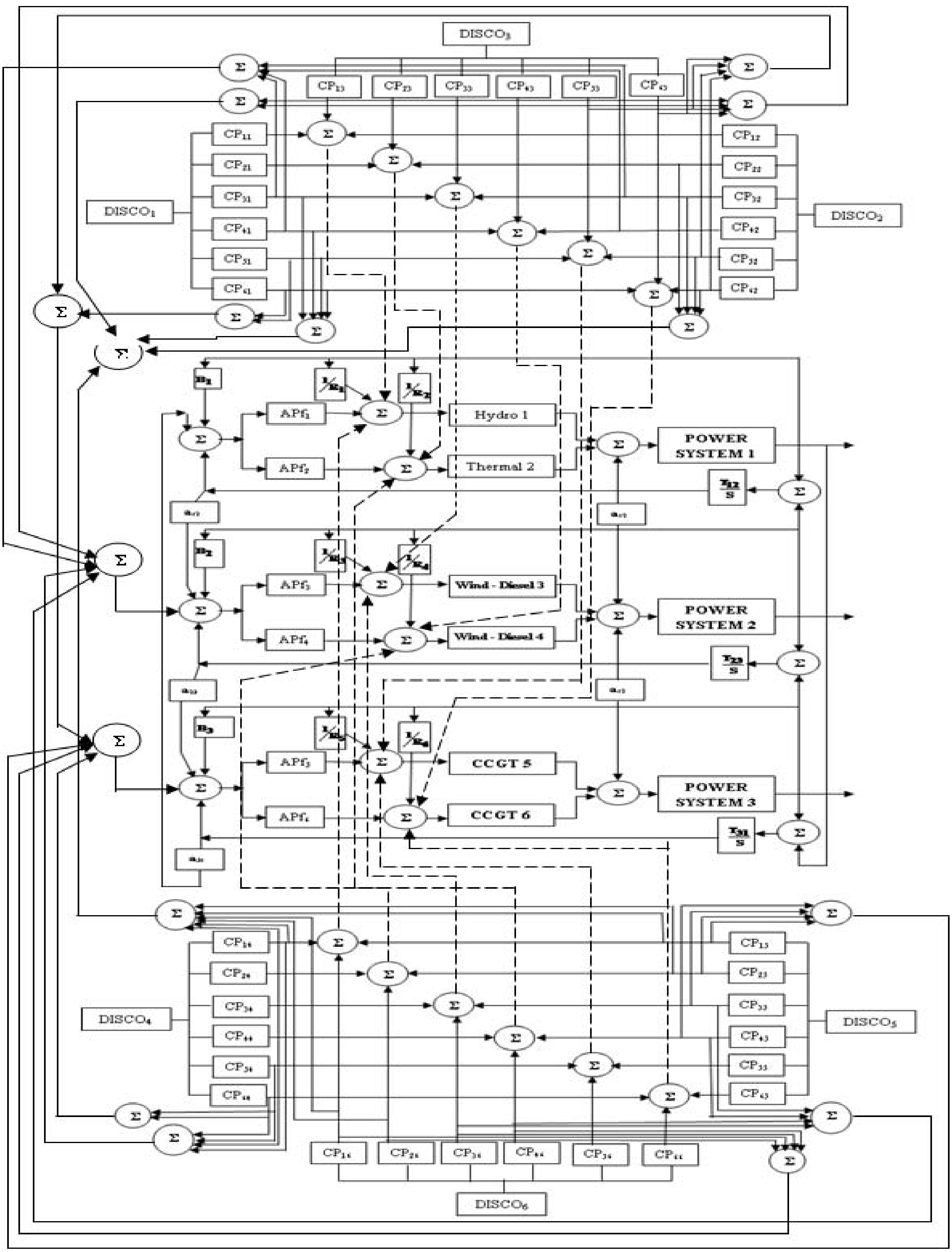

Fig. 6 : Transfer Function Model of Three Area H-T, CCGT & W-D System under Deregulated Environment using SMES/CES

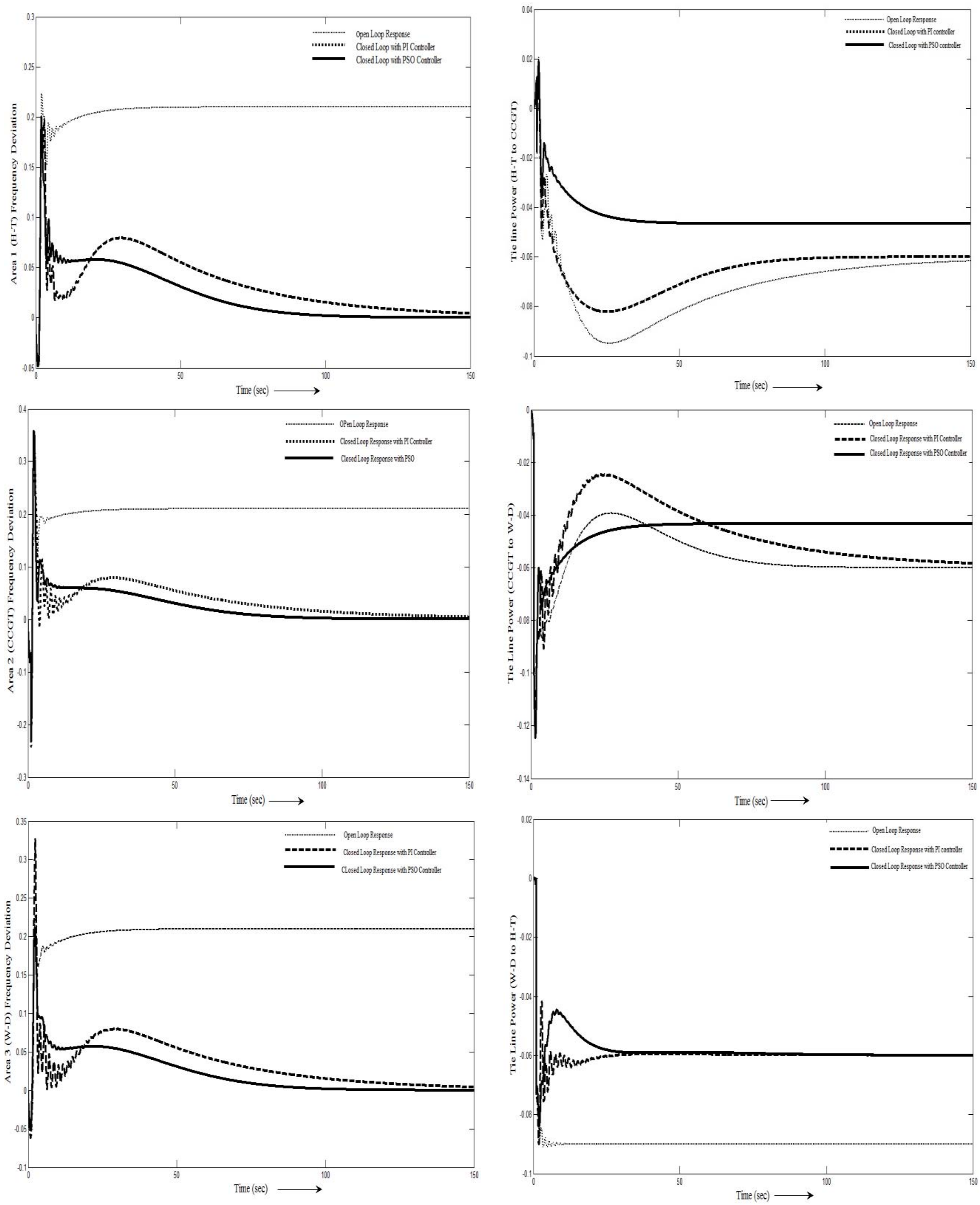

(a) Frequency Deviation

(b) Tie Line Power

Fig. 7 : Comparative analysis of Three area H-T, CCGT & W-D under deregulated Environment without controller, with PI controller & PSO optimized controller

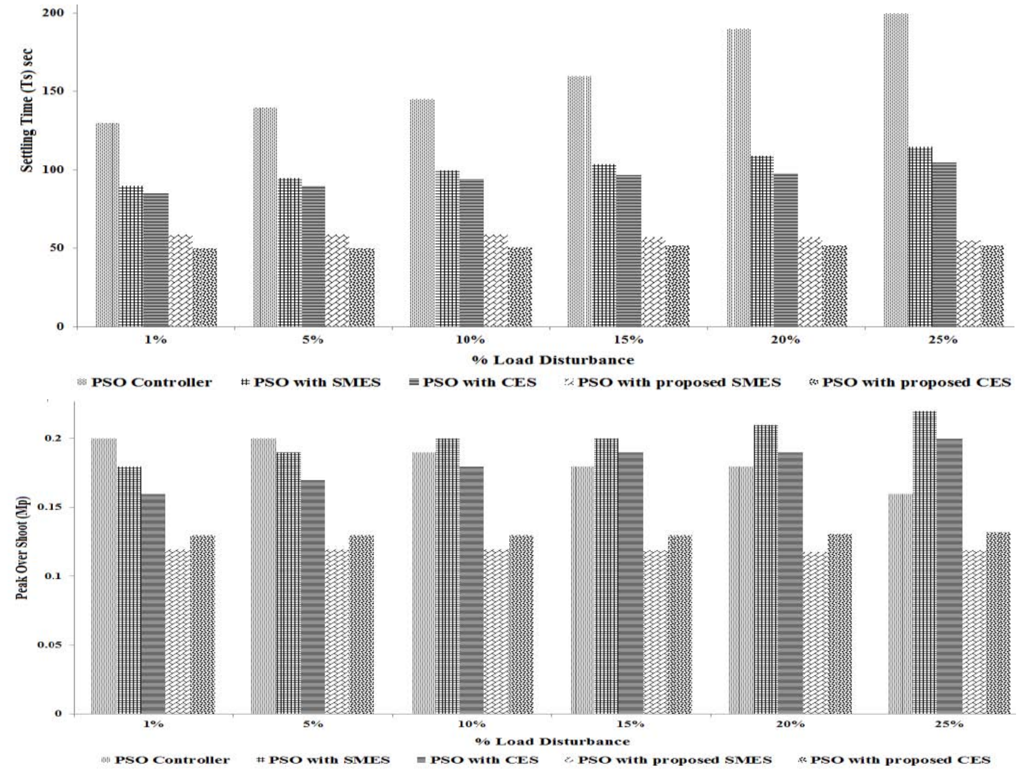

(a) Hydro -Thermal

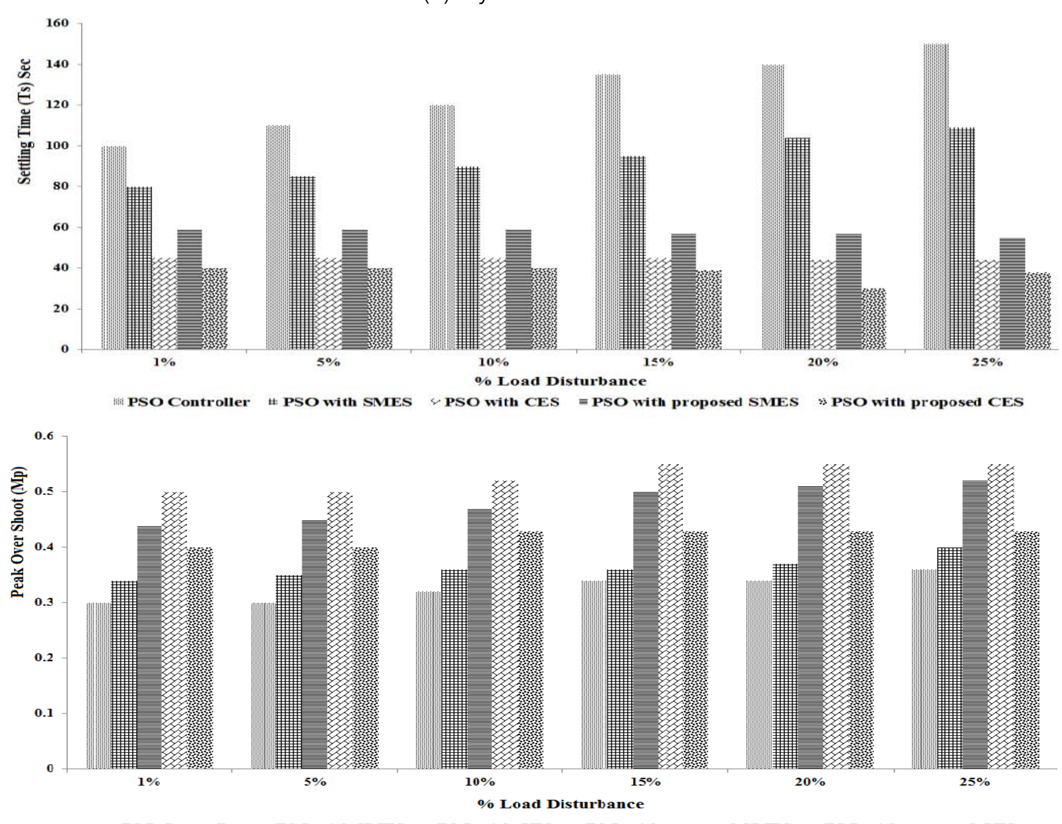

(b) Combined Cycle Gas Turbine

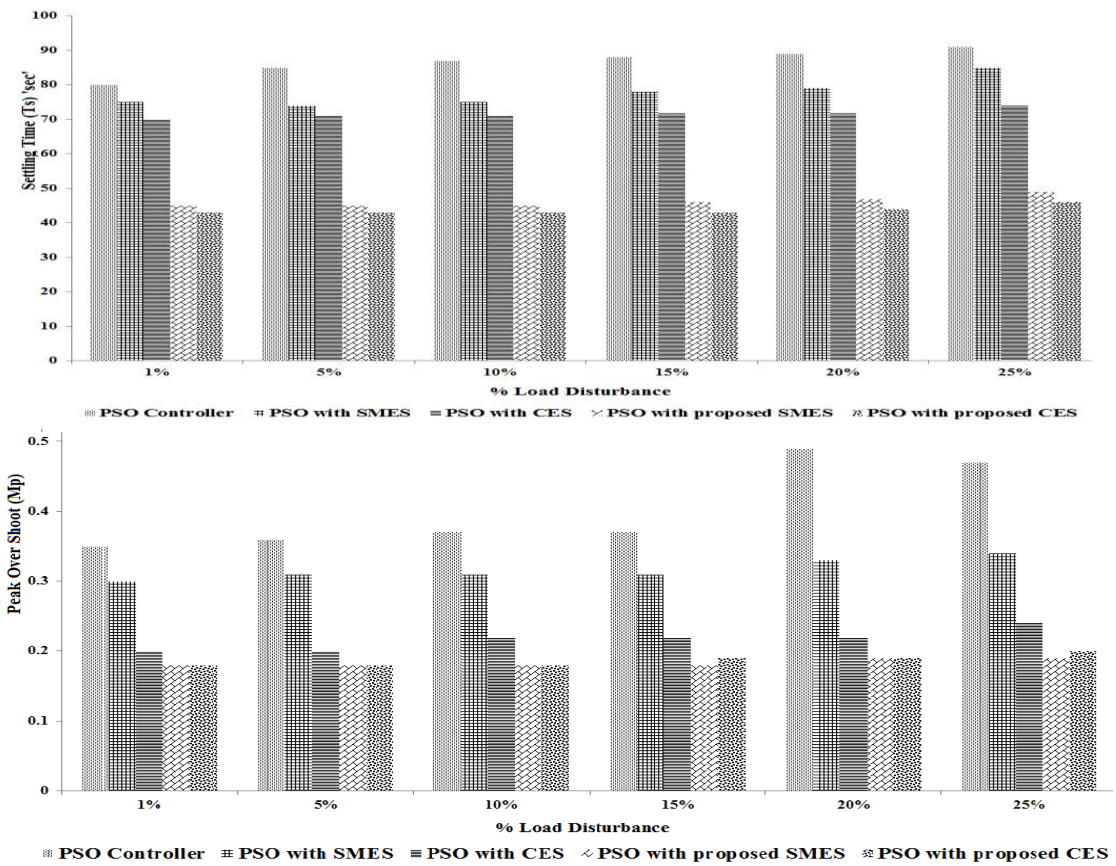

(c) Wind-Diesel

Fig. 8 : Ts and Mp Comparison of Three Area Deregulated H-T, CCGT & W-D System for Different Controller with 25% Load Variations

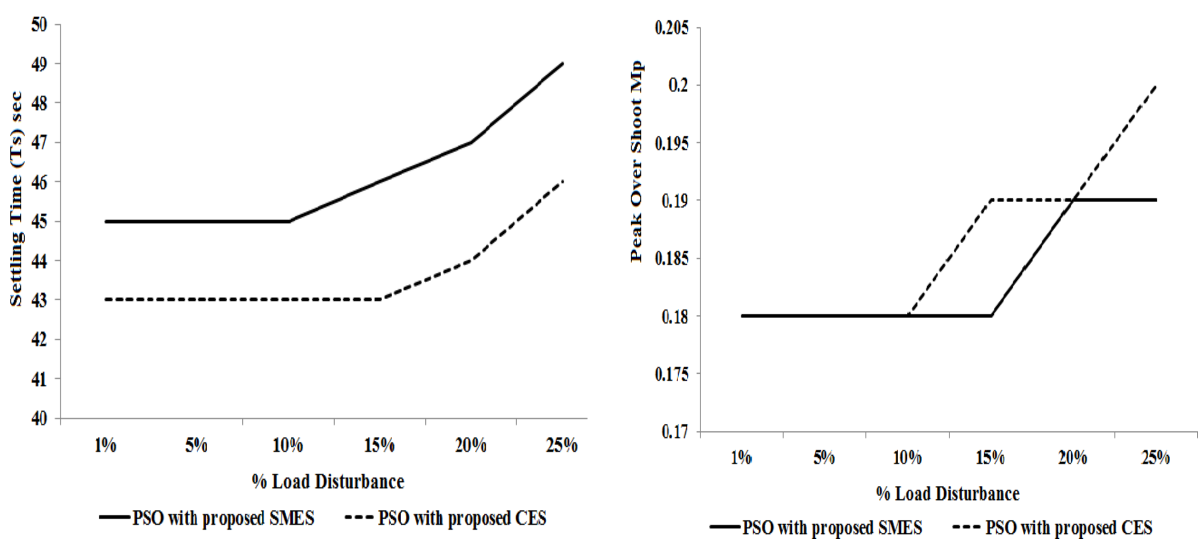

(a) (b)

Fig. 9 : Settling Time & Peak Over Shoot Comparison Between Proposed CES & SMES under Various Load Conditions